



# Thoracic Involvement of Sarcoidosis in Computed Tomography: Radiological Manifestations and Key Findings

Compromiso torácico de la sarcoidosis en tomografía computarizada: claves clínicas y radiológicas

Felipe Aluja Jaramillo<sup>1</sup>  
Alejandra Mendoza Guerra<sup>2</sup>  
Alfonso Lozada Medellín<sup>3</sup>



## Key words (MeSH)

Multidetector computed tomography  
Radiography, thoracic  
Sarcoidosis  
Sarcoidosis, pulmonary

## Palabras clave (DeCS)

Tomografía computarizada multidetector  
Radiografía torácica  
Sarcoidosis  
Sarcoidosis pulmonar

## Summary

Sarcoidosis is a chronic, multisystemic disease of unclear etiology. The presentation is variable according to the geographical origin of the patient, predominantly in Afro-descendant and Scandinavian patients. Chest abnormalities are very frequent in patients with sarcoidosis, taking into account that the most common involvement is lymphatic and the least common is heart involvement. The most frequent radiological manifestations in thoracic involvement due to sarcoidosis are hilar and mediastinal adenomegalies as well as pulmonary nodules with perilymphatic distribution.

## Resumen

La sarcoidosis es una enfermedad crónica y multisistémica de etiología poco clara. La presentación es variable de acuerdo con la procedencia geográfica del paciente, pero predomina en personas afrodescendientes y escandinavas. Las anomalías torácicas son muy frecuentes en los pacientes con sarcoidosis; la afectación más común es ganglionar y la menos común es la del corazón. Las manifestaciones radiológicas más frecuentes en el compromiso torácico por sarcoidosis son las adenomegalias hiliares y mediastinales, así como nódulos pulmonares de distribución perilinfática.

## Introduction

Sarcoidosis is a chronic, multisystemic, inflammatory disease of unclear etiology, mostly seen in African-American women and individuals in the third decade of life (1).

The presentation is variable according to the geographic origin of the patient. In the United States, the annual incidence in the African-American population is 35.5 cases versus 10.9 in Caucasians per 100,000 inhabitants (2). African-American and Scandinavian populations have a higher frequency of sarcoidosis, whereas it is rare in Asia or South America (3). People exposed to fires, metal processing, insecticides, insecticides, molds, inorganic particles, and agricultural chemicals have been found to be at increased risk for sarcoidosis (4).

The pathogenesis is not entirely clear; however, CD4+ T lymphocyte activation and recruitment, macrophage accumulation, and the development of sterile noncaseating epithelioid granulomas have been found to be involved with high interferon- $\gamma$  expression in active sarcoidosis (1). Necrosis is rare in sarcoidosis, with the exception of a variant called necrotizing sarcoid granulomatosis (4). Thoracic abnormalities are evident in more than 90% of patients with sarcoidosis (5), and of these, the most common involvement is in the mediastinum and the least common is that of

the heart, but with higher morbidity and mortality rates compared to pulmonary involvement (1, 4).

Up to 50% of patients are asymptomatic and imaging abnormalities are detected incidentally on chest radiography performed for a different indication (1). Symptoms of pulmonary sarcoidosis include cough, dyspnea and chest pain. Pulmonary sarcoidosis can be difficult to evaluate, because symptomatology, radiological findings and pulmonary function test results can be discordant with each other (6).

The most frequent radiological manifestations in thoracic involvement by sarcoidosis are hilar and mediastinal adenomegalies, and nodules of perilymphatic distribution (3); however, there are atypical presentations of the disease that must be taken into account for an accurate differential diagnosis. The final diagnosis of pulmonary sarcoidosis is established when compatible clinical and radiological findings are found, supported by histological evidence of non-caseating or minimally caseating granulomas in a lymphangitic distribution and once other diseases with similar findings are ruled out (7). A high probability diagnosis without histological confirmation is also accepted when compatible clinical and radiological findings are supported by a BAL CD4/CD8 ratio  $> 3.5$  (specificity 93-96% and sensitivity 53-59%) (7).

<sup>1</sup>Physician, Computed Tomography Section, Country Scan LTDA. Department of Radiology, Hospital Universitario San Ignacio, Pontificia Universidad Javeriana. Bogotá, Colombia. ORCID: <https://orcid.org/0000-0002-3093-2509>

<sup>2</sup>General Physician, Universidad del Rosario. Bogotá, Colombia. ORCID: <https://orcid.org/0000-0001-6773-7064>

<sup>3</sup>Physician, Department of Radiology, PET-CT Unit, Clínica del Country. Department of Radiology, Hospital Universitario San Ignacio, Pontificia Universidad Javeriana. Bogotá, Colombia. ORCID: <https://orcid.org/0000-0003-1329-8769>

The purpose of this review is to describe the epidemiology, pathophysiology and typical and atypical radiological findings of thoracic sarcoidosis on conventional radiology, computed tomography and positron emission tomography.

## 1. Radiologic staging of sarcoidosis in the thorax

Several radiographic staging systems have been established for sarcoidosis. The most widely used was developed by Scadding more than five decades ago (1961) (4,8-10) and modified by DeRemee in 1983 (7, 8) (Table 1). This classification is described for use in chest radiography (RT).

**Table 1. Radiological classification of thoracic sarcoidosis**

Stage	Manifestations	Frequency (%)
0	Absence of abnormalities on chest radiographs.	0-15
I	paratracheal and aortopulmonary window adenomegaly.	25-65
II	Bilateral hilar adenomegaly and pulmonary parenchymal involvement with a bilateral symmetric nodular or reticulonodular pattern with predominant perihilar distribution, in the middle lobe and upper lobe.	25-65
III	Pulmonary parenchymal involvement without hilar adenomegaly.	10-15
IV	Fibrosis with evidence of reticular pattern, traction bronchiectasis, masses causing distortion of architecture or "honeycomb" cysts, predominantly in the upper lobes.	5

Source: Silva et al. (8).

The staging system is interesting from a historical point of view. The distribution of patients according to radiographic stages depends largely on geographical or ethnic origin, as well as on the referral source (9). In general, the percentage of patients diagnosed in stage 0 is 5-15 %, stage I 25-65 %, stage II 20-40 %, stage III 10-15 % and stage IV approximately 5 % (9). It is worth mentioning that symptomatology is not related to the radiographic stage of the disease (5), since this classification scheme is purely descriptive and is not indicative of disease activity (11). Despite the nomenclature, patients do not usually progress through the described stages in a sequential order (12). That is, a patient may present at stage III and during follow-up progress to stage 0. On the other hand, a patient who initially presents with stage I disease may later arrive with parenchymal disease only (stage III). However, this classification has poor reproducibility and interobserver agreement, which limits its daily use (10). Its use has also been restricted because multidetector computed tomography (MDCT) is a more useful modality for the diagnosis and follow-up of sarcoidosis (5). This classification can be extrapolated to be applied in MDCT (Figure 1).

Treatment is considered for symptomatic patients who have relevant findings (hilar or mediastinal adenomegaly, pulmonary pa-

renchymal disease, pulmonary fibrosis, arrhythmias, congestive heart failure, sudden death, among others) in examinations such as radiological, serological, endoscopic, echocardiographic and pulmonary function tests (6). Asymptomatic patients with stage 0 or I disease often do not require management (6). Asymptomatic patients with stage II-III disease, mild functional abnormalities and stable clinical parameters may not require treatment initially and could be followed for up to 3 years (6).

The International Labor Organization (ILO) radiographic scoring system, originally developed for pneumoconiosis, has been modified and applied to sarcoidosis (10). At

this system, shadows are classified into four subtypes (R: reticulonodular; M: mass; C: confluent; or F: fibrosis), which are assigned a score based on extent and profusion separately (10). The Muers classification is derived from the International Labor Organization (ILO) radiographic scoring system for pneumoconiosis and has a higher agreement compared to the Scadding score (8).

MDCT, especially high-resolution chest tomography (HRCT), is the modality of choice for assessing the features of thoracic sarcoidosis. This technique allows the determination of the characteristic features in pulmonary, lymph node, pleural and airway involvement. In addition, MDCT allows the evaluation of possible complications or concomitant entities such as infection or neoplasia (4).

## 2. Manifestations in the mediastinum

### 2.1 Classic presentation

Mediastinal adenomegalies are frequent in patients with sarcoidosis, especially in the right paratracheal station and in the aortopulmonary window (4). One of their main characteristics is that adenomegalies are symmetrical and do not compress adjacent vascular structures (4), which helps to differentiate them from other entities (for example, lymphoma, metastasis or infectious diseases such as tuberculosis) (13). More than 85% of patients with sarcoidosis present with adenomegaly at some point during the course of their disease (5). Approximately 80% of patients with adenomegaly have parenchymal disease and, in turn, more than 80% of patients with pulmonary abnormalities have mediastinal adenomegaly (5).

In all imaging methods it is characteristic that adenomegalies are bilateral and symmetrical (4, 5). In chest radiography, bilateral hilar involvement is the most characteristic pattern - up to 95% of patients - with a typical distribution, called "1-2-3", because it involves bilateral hilar and right paratracheal lymph nodes (5). Additional studies have shown that the most common pattern shows adenomegaly in the aortopulmonary window, right paratracheal and bilateral hilar lymph node stations, a pattern known as the "1-2-3-4" (1).

In 75-95% of patients with sarcoidosis, there are findings of mediastinal and hilar adenomegaly with subcarinal and paraesophageal involvement -each in approximately 50% bilateral hilar in 67%-75% of cases in MDCT (5) (figure of patients- (4,5). MDCT may show adenomegaly 2). The commonly compromised lymph node stations are: mediastinal in the absence of hilar adenomegaly up to 15% right paratracheal and right peribronchial -at least 55%-70% of patients (5)

## 2.2 Atypical presentation

Sarcoidosis may manifest as asymmetric or unilateral mediastinal or hilar adenomegaly, so differential diagnoses must be taken into account, for example: lymphoma, neoplastic involvement, tuberculosis or even other granulomatous disorders (4). Unilateral

involvement has been described, especially right, in 5% of patients (14). Likewise, unusual localizations -such as in the internal mammary and retrocrucl lymph node stations- are considered atypical presentations of the disease (Figure 3) (5, 14).

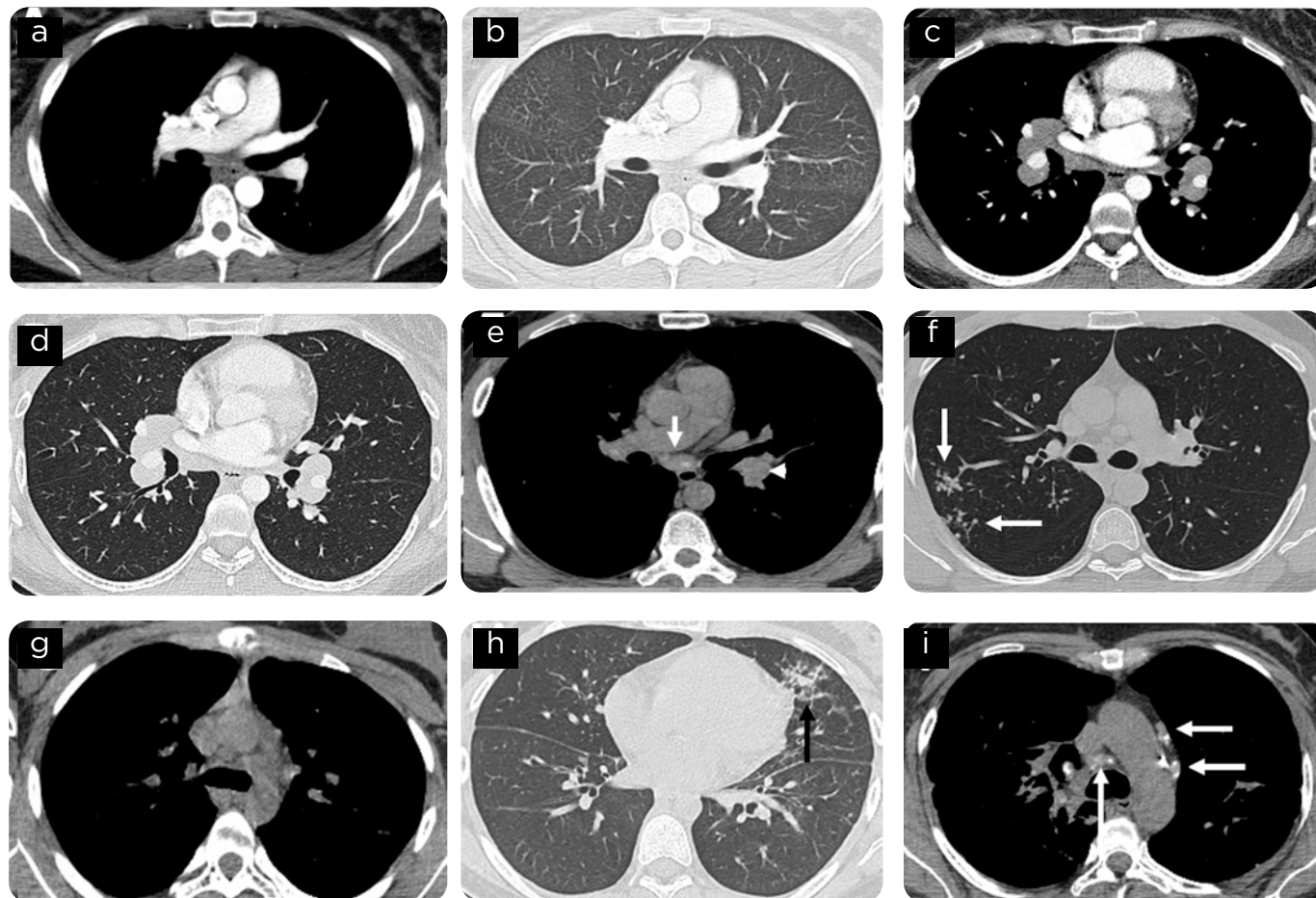


Figure 1. Chest CT findings in patients with different forms of presentation of sarcoidosis to extrapolate of sarcoidosis for extrapolation of the classification of thoracic sarcoidosis. 24-year-old patient with a diagnosis of sarcoidosis with diagnosis of sarcoidosis: a) CT in mediastinal window and b) lung, no abnormalities are identified. abnormalities are not identified. 38-year-old patient with a diagnosis of sarcoidosis: c) CT scan of the thorax, window for mediastinum and b) lung. c) Chest CT, mediastinal window, multiple symmetrical and well-defined hilar adenomegalies are observed. d) Chest CT, lung window, no abnormalities are identified. Patient of 28 years old 28 years old with a diagnosis of sarcoidosis: e) CT scan of the chest, mediastinal window, some adenomegalies are: mediastinal adenomegaly predominantly hilar and infracarinal (arrow) and f) CT scan of the chest, window for lung, some solid, rounded nodules are observed in perilymphatic and centrilobular distribution (arrow). perilymphatic and centrilobular distribution in the posterior segment of the right upper lobe (arrow). Patient 36 years old with a diagnosis of sarcoidosis: g) Chest CT scan, mediastinal window, no abnormalities were abnormalities are observed and h) CT of thorax, window for lung, some solid, rounded nodules are observed, rounded, in distribution rounded solid nodules in perilymphatic distribution and areas of "ground glass" in the lingula (arrow). (arrow). 63-year-old patient with diagnosis of sarcoidosis: i) Chest CT scan, window to mediastinum, multiple adenomatous mediastinum, multiple mediastinal adenomegalies, some of them calcified (arrow) and j) chest CT, window for mediastinum. (j) Chest CT, lung window, pulmonary architecture alteration with reticulation and perilymphatic nodules (arrow). and perilymphatic nodules

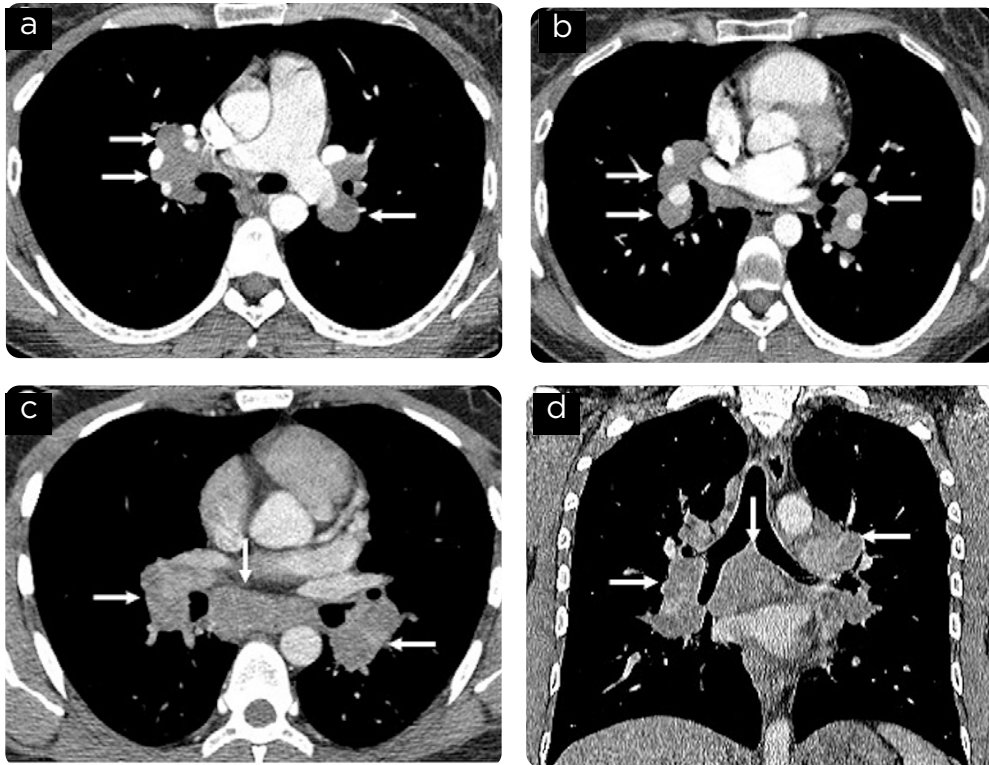


Figure 2. 48-year-old patient with diagnosis of sarcoidosis. Chest CT with contrast medium, mediastinal window: a) at the level of the pulmonary artery and b) in the lower lobes. Multiple symmetric and well-defined hilar adenomegalies predominating in the parahilar region (arrows). 44-year-old patient with a diagnosis of sarcoidosis. Chest CT with contrast medium: c) mediastinal window in inferior lobes, d) coronal reconstruction. Multiple symmetric and well-defined mediastinal and hilar adenomegalies predominating in the parahilar region (arrows).

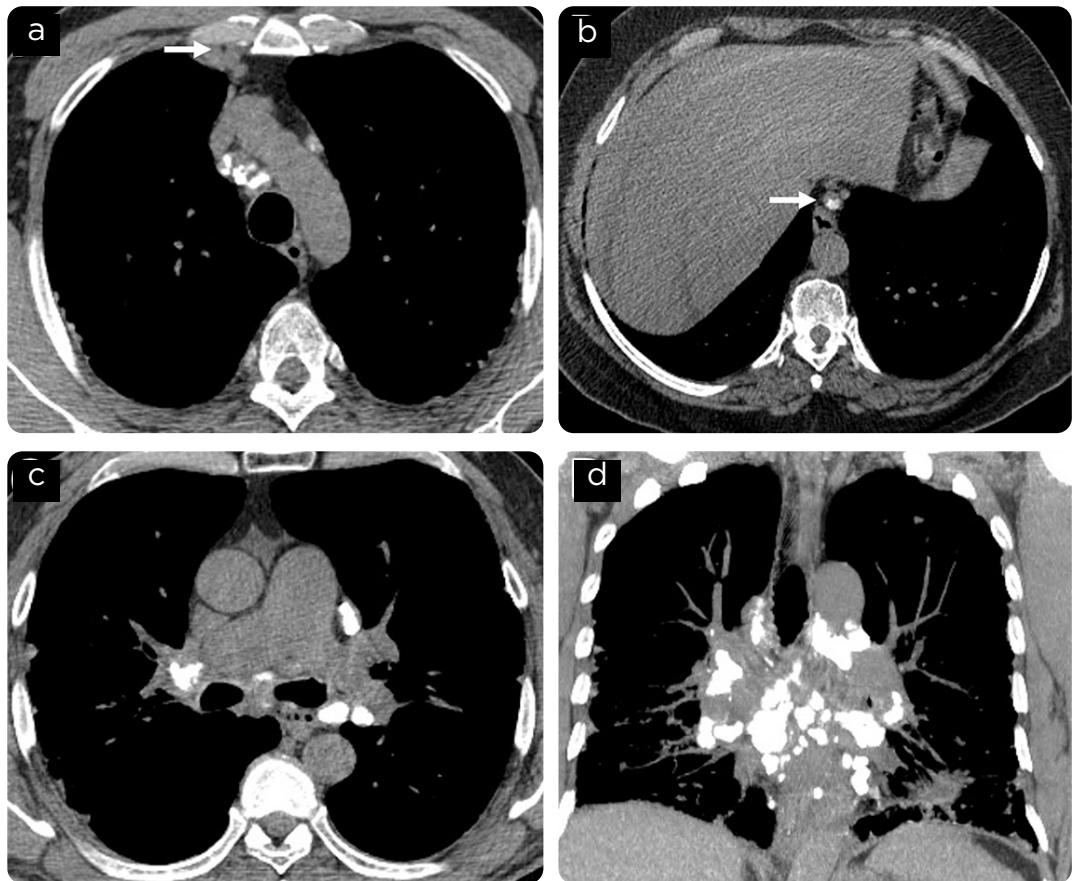


Figure 3. 67-year-old patient with diagnosis of sarcoidosis. Chest CT, mediastinal window: a) at the level of the aortic arch and b) at the gastroesophageal junction. Calcified mediastinal adenomegaly of atypical location, in the right internal mammary chain, in a, and adjacent to the gastroesophageal junction, right paratracheal and prevascular in b, are observed. 64-year-old patient with a diagnosis of sarcoidosis. Chest CT, mediastinal window: c) at the level of the pulmonary artery and d) coronal reconstruction. Multiple mediastinal and hilar calcified adenomegalies are observed in a patient with a history of sarcoidosis of several years of evolution confirmed by biopsy.

Adenomegalies are frequently calcified (figure 3); they can be found with focal or diffuse calcifications and with variable patterns: amorphous, dotted, dense and thick, or in “eggshell” (5), a finding that is closely related to the duration of the disease (1). Focal calcifications are more frequent than complete calcifications of adenomegaly (1). As an additional fact, on magnetic resonance imaging (MRI), a low signal adenomegaly on T1- and T2-weighted sequences, called “dark lymph node”, is a sign that can be found in up to 50% of patients with sarcoidosis (5). Calcifications of adenomegaly are more frequent in patients older than 50 years (14, 15).

### 2.3 Mediastinal complications

Pulmonary arterial hypertension (PAH) is a widely described complication of sarcoidosis, called sarcoidosis-associated pulmonary hypertension (1), which is independent of pulmonary fibrosis (13, 16). It occurs in 5% to 74% of patients with sarcoidosis, with a 5-year survival of approximately 59%. The diagnosis, as in other forms of PHT, is made when a dilatation of the main pulmonary artery exceeding 29 mm in transverse diameter is found (4). In addition, it is important to obtain the radius between the pulmonary artery and the ascending aorta, which must be greater than 1, to make the diagnosis; furthermore, it has a predictive value for mortality independent of other factors found in MDCT (17). Anatomopathological studies have shown granulomatous invasion of blood vessel walls or perivascular fibrosis, especially in venous vessels, which occurs in 69% to 100% of patients (18, 19). However, it is rare to find PHT changes in patients with sarcoidosis without pulmonary fibrosis and secondary to thrombosis or occlusive compromise of venous vessels (20, 21). As mentioned, its etiology is multifactorial (22) and, therefore, it is part of group 5 of the classification of pulmonary arterial hypertension (23, 24).

## 3. Manifestations in the lung parenchyma

### 3.1 Classic presentation

The pulmonary involvement of sarcoidosis is varied, characterized by nodules and masses found in approximately 15% to 25% of patients (1). Chest radiography shows pulmonary involvement by nodules in approximately 50% of cases (5). In MDCT, nodules are solid, well defined, tend to measure between 2 to 5 mm, their distribution is predominantly perilymphatic (75 % to 90 % of cases) (14, 25), so they are found in the interlobular septa, in the peribronchovascular interstitium, the cisuras and subpleural regions with predominance in upper lobes and middle lobe (figure 4) (4, 26). The distribution of these nodules can be in “patches”, located in areas of compromised lung intermingled with areas of normal lung (5). These nodules may confluence to form larger nodules or masses (27,28), simulating areas of consolidation or progressive massive fibrosis. Perihilar and peribronchovascular opacities have also been described extending from the pulmonary hilar to the periphery with or without air bronchogram, more profuse towards the central zone, usually accompanied by nodules (figure 5) (4, 5).

Sarcoidosis can follow two paths: the first is spontaneous regression of the disease and its manifestations; the second is progression of the disease to pulmonary fibrosis. Uncontrolled inflammation

usually precedes fibrotic change, and up to 20% of patients with sarcoidosis develop pulmonary fibrosis (14, 29, 30). The mechanisms of the disease are not yet fully understood, although a complex interaction of multiple factors appears to be at play, including genetics, CD4+ T cells, and cytokines such as TNF- $\alpha$ . Pulmonary fibrosis corresponds to stage IV. The development of pulmonary fibrosis is associated with significant morbidity and can be fatal (31-33) or even require lung transplantation (34). Dyspnea, cough and hypoxemia are common clinical manifestations (31). Pulmonary function tests often show restriction of parenchymal involvement, although air-flow obstruction due to airway-centered fibrosis is also recognized (31). It should be emphasized that fibrosis often remains stable for prolonged periods, making it difficult to assess disease activity (6). It is important to differentiate reversible granulomatous disease from fibrosis (irreversible changes), since the treatment of sarcoidosis is based on the assumption of reversible granulomas (25,31). In this context, 18-Fluorodeoxyglucose (18-Fluorodeoxyglucose (18-FDG) PET/CT is useful to evaluate active inflammation indicating reversible granuloma (6).

A persistent reticular pattern on chest radiograph is indicative of fibrosis. This reticulation and fibrosis tend to be irregular, but predominant in the upper lobes (1). Progression of pulmonary fibrosis produces volume loss, typically of the upper lobes, and superior retraction of the pulmonary hilum which can be identified on chest radiography. Traction bronchiectasis and architectural distortion are commonly seen. Continuous fibrosis may become confluent and give rise to mass-like peribronchovascular fibrous tissue, simulating the appearance of progressive massive fibrosis seen in silicosis (1).

MDCT is a useful tool in the evaluation of patients with sarcoidosis lung disease (Figure 6) (25). The most common finding is pseudomas in upper and middle lobes associated with reticulation, altered pulmonary architecture and traction bronchiectasis with a predominantly patchy distribution (6, 14). The findings of pulmonary fibrosis in sarcoidosis differ from the patterns of idiopathic pulmonary fibrosis, due to their distribution and the uniformity of fibrosis changes in the latter (35-37).

### 3.2 Atypical presentation

Because of the possible atypical presentations, sarcoidosis has been called “the great simulator”. Due to its characteristics, the differential diagnosis can be broad considering lymphangitic dissemination, expositional lung disease, progressive massive fibrosis, hypersensitivity pneumonitis and Langerhans cell histiocytosis, among others (13, 38).

The nodules when confluent can form a mass (or larger nodule) surrounded by smaller nodules in its periphery (satellite nodules), which has been called the “galaxy” sign (1, 14, 39), which is not specific to the disease, and has been described in other granulomatous and neoplastic entities (1, 14). Solitary nodules or masses are rarely found in the context of a patient with sarcoidosis (40). Likewise, multiple larger nodules, usually larger than 5 mm, can simulate secondary neoplastic involvement (Figures 7 and 8) (14). Another form of presentation described is the “sarcoid cluster”, which represents a group of nodules of peripheral predominance that can be of rounded or oval morphology (41).

Consolidations are evident in 10% to 20% of patients with sarcoidosis (Figure 9) (14). They are bilateral, symmetrical and of peribronchovascular distribution with a predominance towards the upper and middle lobes (14). In these cases it is frequent to find areas of air bronchogram, which gives an appearance even more similar to a consolidation (5).

Ground-glass opacities can be found on MDCT in up to 40% of patients (Figure 10) (5, 14); however, the frequency of this finding in sarcoidosis is variable (5). The distribution may be patchy and is rarely extensive (14). These areas reflect the presence of numerous small granulomas and interstitial fibrous lesions that cause airway compression without alveolar occupation (14). The areas of “ground glass” may be related to areas of nodularity of the underlying pulmonary parenchyma (14).

The “miliary” pattern is rare in sarcoidosis and has been documented in less than 1% of patients (14). When it is found, in the first instance it is necessary to rule out tuberculosis, metastatic disease or even occupational lung disease (14).

Air trapping in MDCT during expiratory acquisitions is also frequently seen in sarcoidosis (Figure 11) (1). Pulmonary fibrosis may occur in 20% to 25% of patients with sarcoidosis, which characteristically predominates in the upper and middle lobes (4). On some occasions, the nodules confluence to form larger masses. Pulmonary aspergillosis superinfection and mycetoma formation may develop in up to 2% of sarcoidosis patients, especially in those with pulmonary fibrosis, cystic lung disease, pre-existing pulmonary cavitations and bronchiectasis (4).

## 4. Airway manifestations

### 4.1 Tracheobronchial tree

Tracheobronchial involvement may also occur, although infrequently, and may pose a diagnostic challenge (4). In the main airway, HRCT may show small granulomas in the tracheal or bronchial walls, wall thickening or irregularity, or focal bronchiectasis (5, 42). Tracheal involvement is not common; however, it can affect segmental and subsegmental bronchi (43). Areas of focal stenosis of the trachea have been described which may be secondary to extrinsic compression derived from adenomegaly in the mediastinum (43). Likewise, in MDCT, areas of stenosis of the airway with nodular or smooth appearance can be found (figure 12) (43). The decrease in the caliber of the segmental bronchi can cause atelectasis, especially in the right middle lobe (1). Bronchial abnormalities consist mainly of nodular bronchial wall thickening or small endobronchial lesions (44).

### 4.2 Small airway

Sarcoidosis may involve the small airways. Granulomas in the small airways may result in air trapping and, as a consequence, show areas of attenuated mosaic attenuation areas more evident on expiratory MDCT. Air trapping is common and may occur in up to 95% of patients (5).

## 5. Pleural manifestations

Pleural involvement has been documented in 1-4% of patients with sarcoidosis (14, 45, 46). Patients may develop plaque-like pulmonary

opacities of subpleural location, caused by subpleural aggregations of small parenchymal nodules called “pseudoplaques”, which have irregular but well-defined margins (5, 14). Pulmonary opacities that simulate pleural plaques have also been described, called “pleural plaque opacities” (Figure 13) (1).

Pleural effusion (hemorrhagic or chylothorax) is a very rare complication and occurs in cases of sarcoidosis as a secondary manifestation to extrinsic compression of mediastinal adenomegalies (14, 47). Pleural effusion, if found, is scarce and usually resolves spontaneously between 2 and 3 months after its appearance (14). Effusions are generally observed in cases with extensive pulmonary or systemic involvement (44). Lymphocytic pleural aspirates,

often blood-stained, are characteristic of involvement (44). A diagnosis can be made when pleural biopsies show non-caseating granulomas without acid-fast bacilli by staining or under culture conditions (44).

Rarely, findings of pneumothorax have been described as complications secondary to rupture of subpleural bullae in patients in fibrotic stages of the disease (14, 45).

## 6. Usefulness of PET/CT in the assessment of thoracic sarcoidosis

Although positron emission tomography (PET-CT) is not included in the standard study for sarcoidosis (8), there is evidence to support the value of this test in guiding the diagnosis and management of these patients. PET-CT has great utility in defining active inflammatory processes (8), it also serves to evaluate reversible granulomas, response to treatment, extent of disease, occult disease, bone or cardiac sarcoidosis, and to determine the most appropriate biopsy site (6). PET is increasingly useful in cases of cardiac involvement in sarcoidosis, to determine the activity of the inflammatory process, since, although clinically it is only detected in approximately 5% of patients, in different series of autopsies such involvement has been found in up to 25% of cases (48). MR and PET imaging have been used in conjunction to determine cardiac involvement, as recommended in the 2014 Heart Rhythm Society expert consensus statement (49). Seventy-three percent of sarcoidosis patients demonstrate disease activity on PET-CT (50). 18FDG-PET identifies clinically silent uptake in 15 % of sarcoidosis patients (8) and its use may guide the identification of biopsy sites for diagnosis in 3.8 % of patients (51). Mediastinal and hilar adenomegalies show increased radiotracer uptake (Figure 14) (2), finding in some cases the “lambda ( $\lambda$ ) sign”, which is described in nuclear medicine images as increased metabolic activity in mediastinal lymph nodes of right paratracheal and bilateral hilar location (52). In the case of the pulmonary parenchyma, detection of pulmonary involvement has been demonstrated in patients after transplantation (53), in the pulmonary nodules of the disease (figure 15) and in consolidations (figure 16). After treatment, a decrease in radiotracer uptake has been observed, which demonstrates its usefulness in the follow-up of the disease (54). It must be taken into account that the main differential diagnosis of sarcoidosis in PET-CT is neoplasia (52), noting that it has been documented that patients with this entity have a 5.5 times higher risk of suffering lymphoproliferative disorders (2).

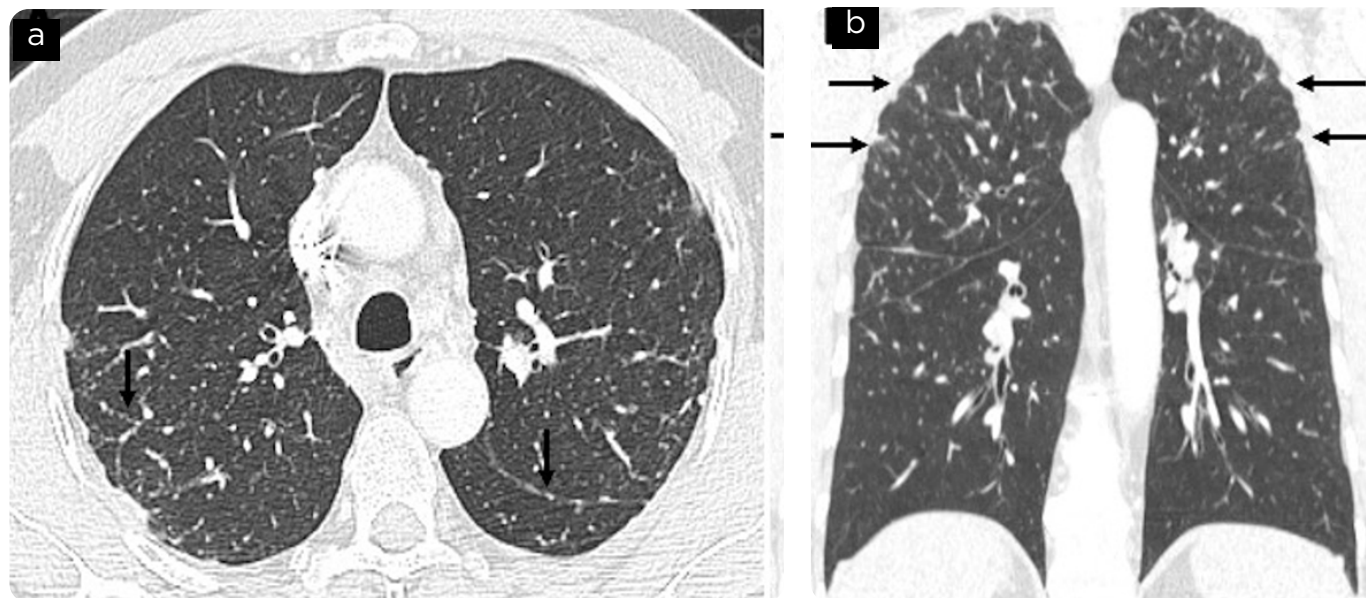


Figure 4. 56-year-old patient with a diagnosis of sarcoidosis. Chest CT, a) lung window and b) coronal reconstruction. There are solid nodules with soft tissue density no larger than 5 mm of perilymphatic disposition (arrows).

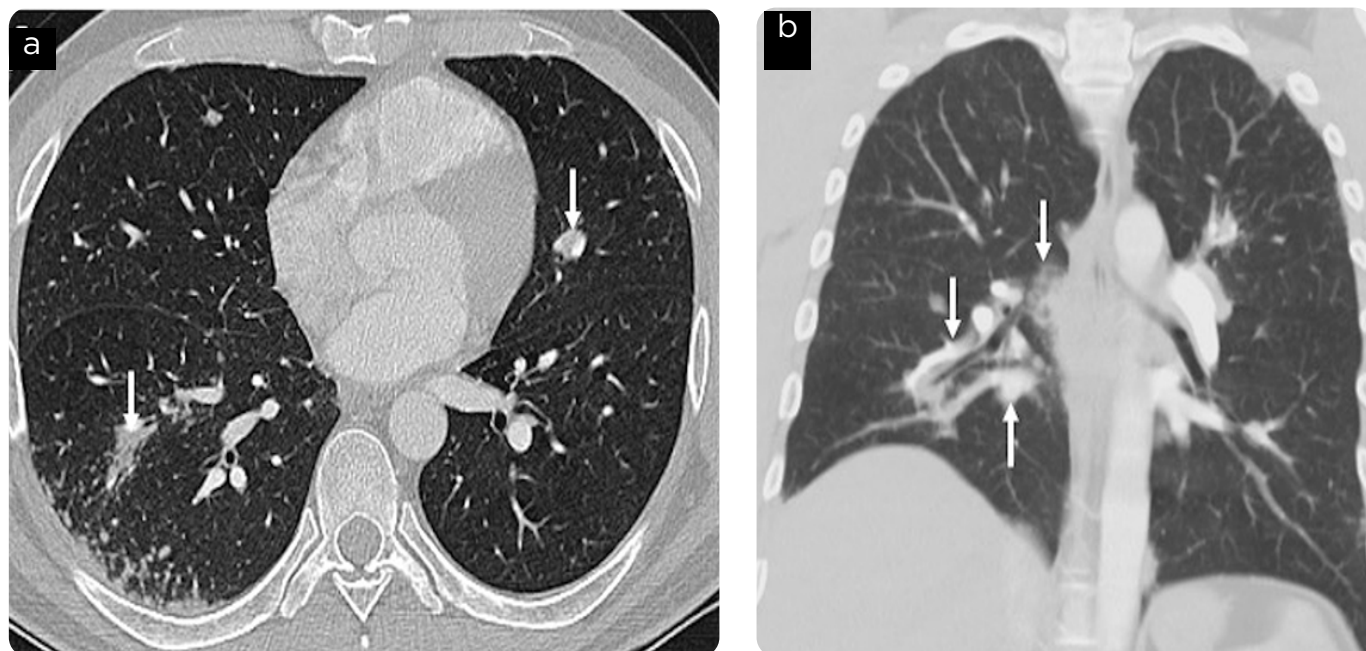


Figure 5. 24-year-old patient with diagnosis of sarcoidosis. Chest CT, lung window in a) lower lobes and b) coronal reconstruction. Peribronchovascular opacities are observed with predominance in the right lower lobe.

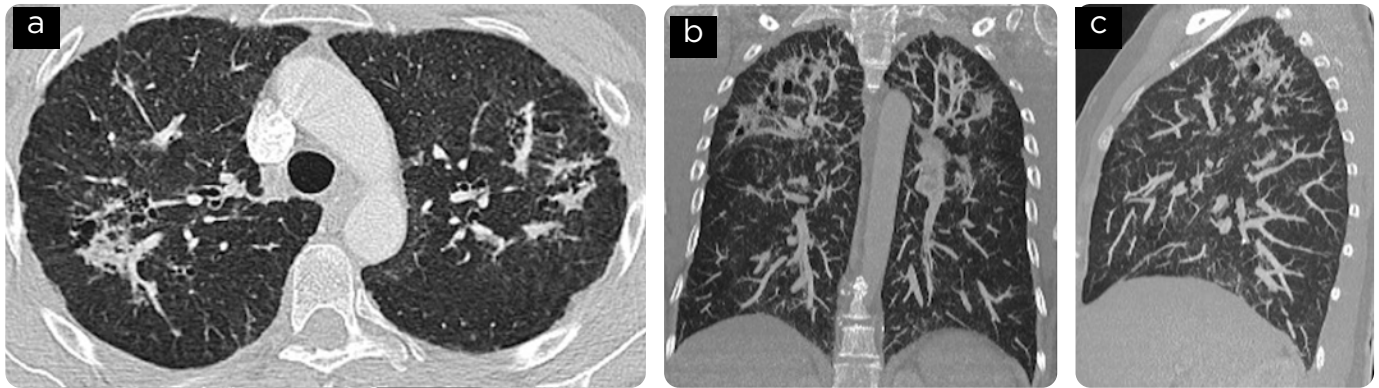


Figure 6. 49-year-old patient with a diagnosis of sarcoidosis of several years of evolution. Chest CT: a) window for lung in upper lobes, b) coronal and c) sagittal reconstruction. Pulmonary architecture alteration is observed with irregular thickening of interlobular septa, bronchiectasis and cavitation areas in the upper lobes due to fibrotic changes.

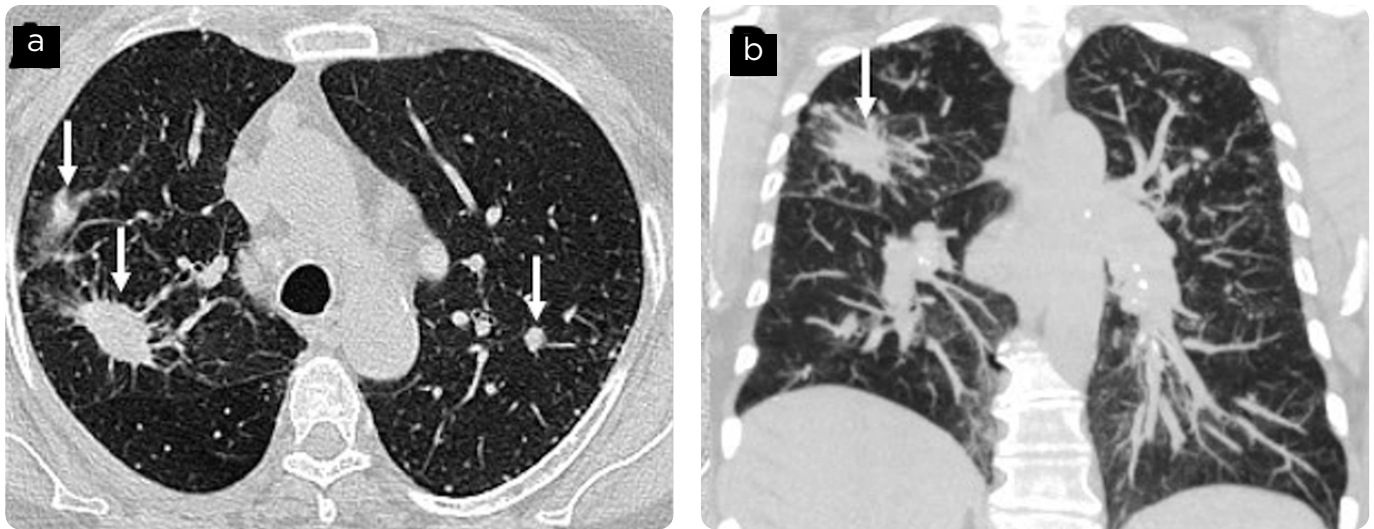


Figure 7. 52-year-old patient with a diagnosis of sarcoidosis. Chest CT, a) upper lobe lung window and b) coronal reconstruction. There is a solid oval nodule with spiculated contours in the right upper lobe (white arrow) and some smaller nodules in the right upper lobe, right lower lobe and left upper lobe. There are also some perilymphatic nodules.

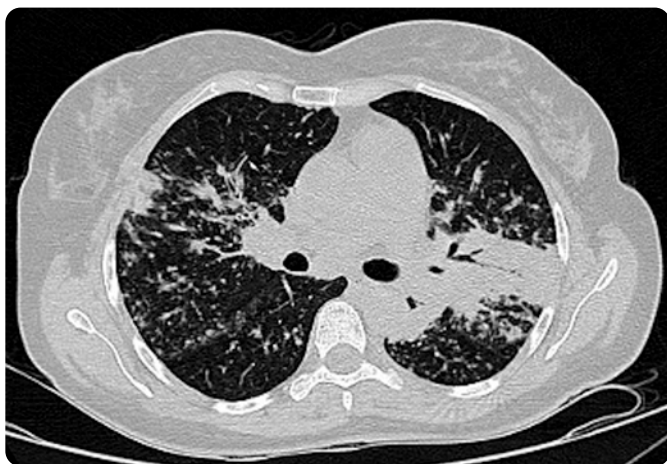


Figure 8. 47-year-old patient with diagnosis of sarcoidosis. Simple CT of the thorax, window for lung below the carina. Bilateral parahilar masses with calcifications inside, bilateral, symmetrical, with air bronchogram. There are associated perilymphatic perilymphatic distribution.



Figure 9. 41-year-old patient with diagnosis of sarcoidosis. Simple CT scan of the chest, lung window. Area of consolidation in the upper segment of the lingula (arrow).

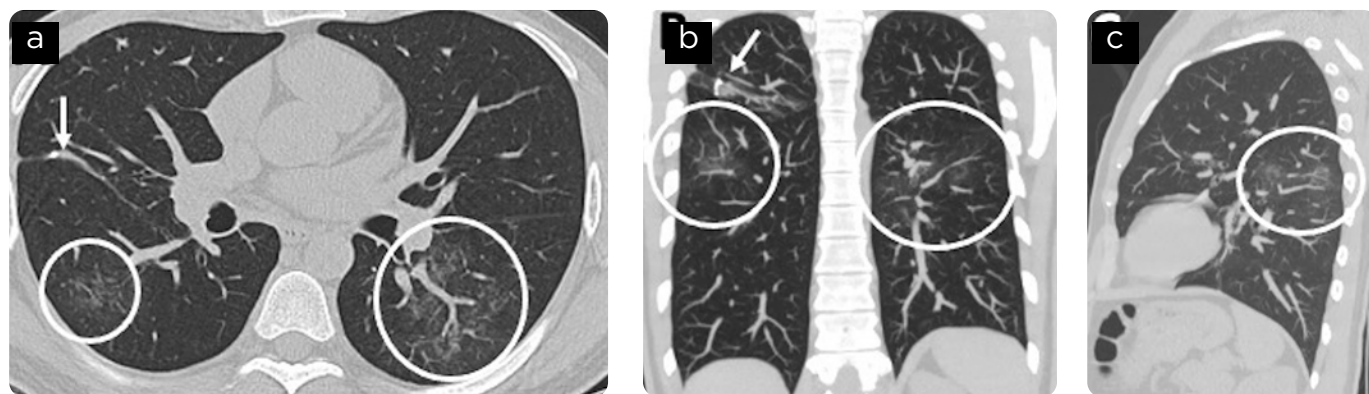


Figure 10. 23-year-old patient with diagnosis of sarcoidosis. Chest CT: a) window for lung in lower lobes, b) coronal and c) sagittal reconstruction. Area of “ground glass” in the left lower lobe in a patient with a proven diagnosis of sarcoidosis. Metallic suture in the right upper lobe and middle lobe (arrow).

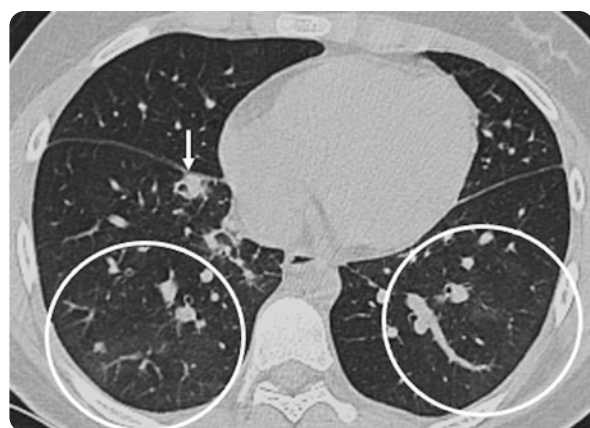


Figure 11. 31-year-old patient with diagnosis of sarcoidosis. Simple CT scan of the chest, lung window. Discrete areas of “ground glass” of geographic arrangement, predominantly in lower lobes compatible with attenuation mosaic secondary to airway compromise. There are some areas of peribronchovascular consolidation (white arrow).

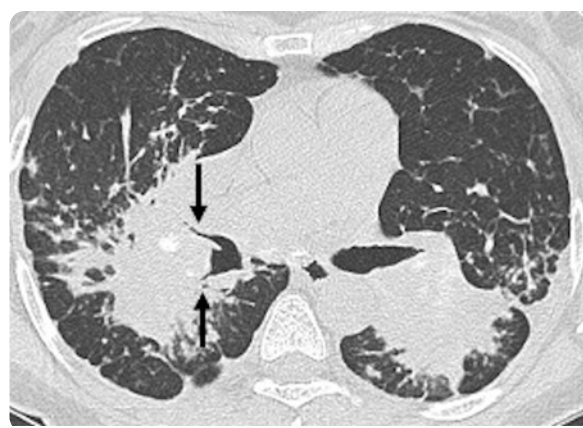


Figure 12. 61-year-old patient with diagnosis of sarcoidosis. Simple CT of the thorax, window for lung in lower lobes. Bilateral parahilar masses with calcifications inside, bilateral, symmetrical, associated with perilymphatic distribution nodules. There is decrease in bronchial caliber for the middle lobe and for the right lower lobe (black arrows), causing almost complete obliteration of the bronchus.

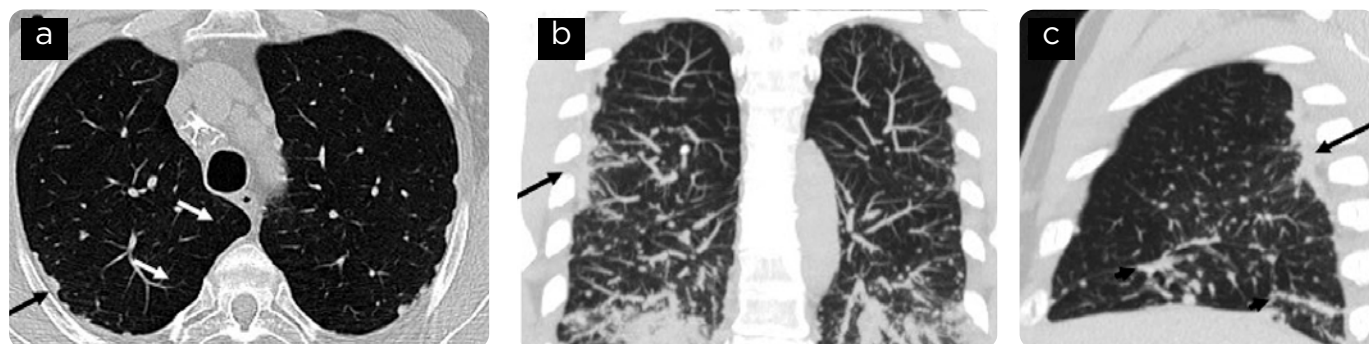


Figure 13. 65-year-old patient with a diagnosis of sarcoidosis. Simple CT of thorax, window for lung: a) in upper lobes, b) coronal reconstruction and c) sagittal reconstruction. Subpleural nodular opacities (white arrow) with soft tissue density, some confluent configuring pleural plaques (black arrow). There are multiple solid nodules of perilymphatic and subpleural predominance in lower lobes (short black arrow in c and d).

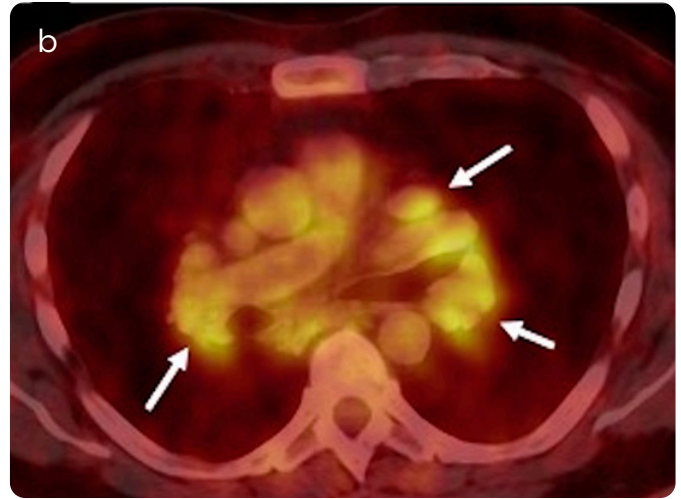
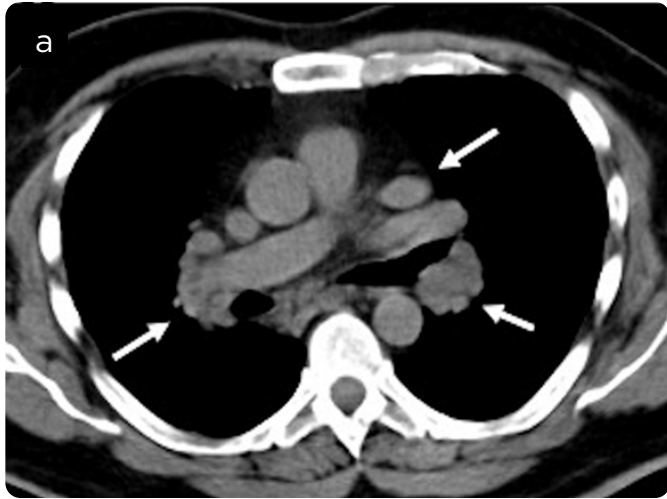


Figure 14. a) Axial images of simple CT for attenuation correction and b) PET-CT fusion. Bilateral hypermetabolic hilar adenopathies are identified (white arrows), in patient with active sarcoidosis.

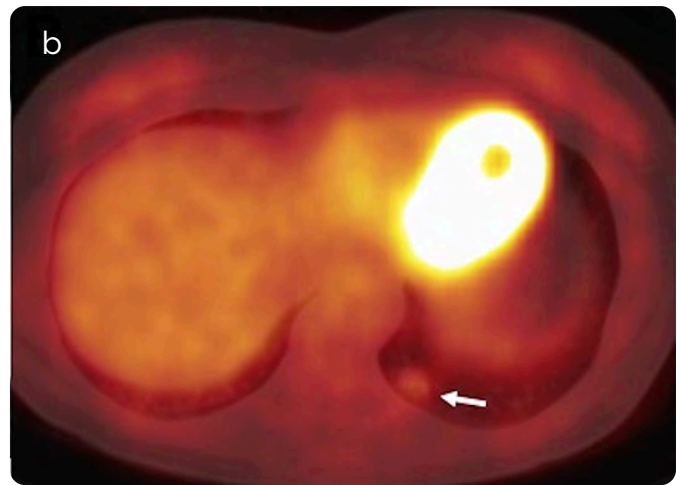
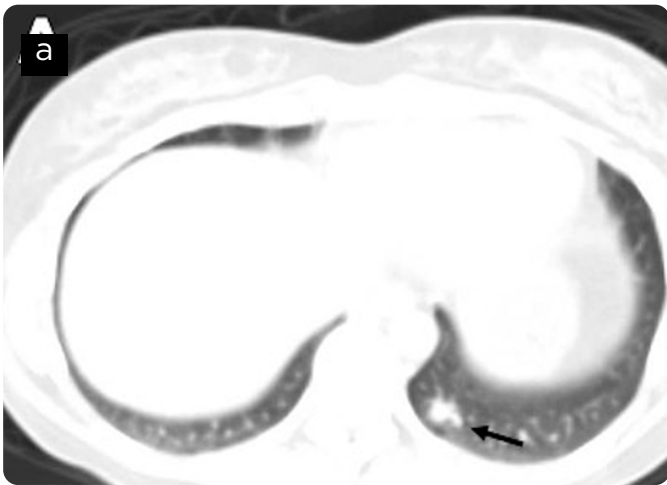


Figure 15. Axial images of simple CT for: a) attenuation correction and b) PET-CT fusion. 42-year-old patient with a history of sarcoidosis: a solid, lobulated and spiculated nodule is found in the posterior segment of the left lower lobe (black arrow), with low metabolic activity (white arrow). Follow-up with high-resolution CT was performed, and complete remission of the nodule was observed at 6 months.

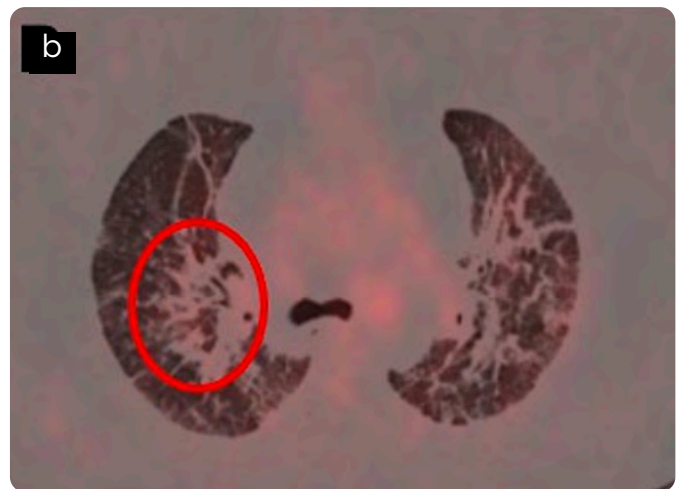
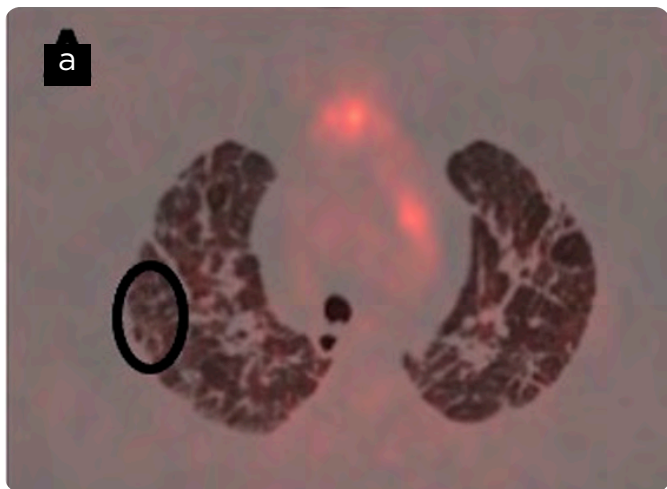


Figure 16. a and b). Axial images of PET-CT fusion. In the upper lobes there are predominantly subpleural reticular interstitial opacities (black ellipse) and peribronchovascular interstitial thickening (red ellipse), in a patient with type IV sarcoidosis, with fibrotic pulmonary changes, without significant increase of metabolic activity in the parenchyma. (Courtesy of Dr. Gabriela Segura, Hospital de especialidades Carlos Andrade Marín, Quito, Ecuador).

## Conclusions

Sarcoidosis is a disease with multiple systemic manifestations, and the thorax is no exception. The most frequent intrathoracic manifestations are bilateral hilar and mediastinal adenomegaly, as well as pulmonary nodules with perilymphatic distribution.

However, there are patients with atypical manifestations or even a smaller percentage with no thoracic manifestations. The spectrum of radiological findings of this disease in the most frequently used imaging methods should be known.

## References

- Lee GM, Pope K, Meek L, Chung JH, Hobbs SB, Walker CM. Sarcoidosis: A diagnosis of exclusion. *AJR*. 2020;214:1-9. doi: 10.2214/AJR.19.21436.
- Prabhakar HB, Rabinowitz CB, Gibbons FK, O'Donnell WJ, Shepard JO, Aquino SL. Imaging features of sarcoidosis on MDCT, FDG PET, and PET/CT. *AJR*. 2018;190:S1-S6. doi: 10.2214/AJR.17.7001.
- Semionov A, Kosiuk J, Ajlan AM, Discepolo F. Thoracic diseases with musculoskeletal manifestations and vice versa: A review. *AJR*. 2018;211:1000-9. doi: 10.2214/AJR.18.19803.
- Ganeshan D, Menias CO, Lubner MG, Pickhardt PJ, Sandrasegaran K, Bhalla S. Sarcoidosis from head to toe: what the radiologist needs to know. *Radiographics*. 2018;38(4):1180-200. doi: 10.1148/rg.2018170157.
- Reddy GP, Ahuja J. Thoracic sarcoidosis: Imaging patterns. *Semin Roentgenol*. 2019;54(1):59-65. doi: 10.1053/j.ro.2018.12.008.
- Akaike G, Itani M, Shah H, et al. PET/CT in the diagnosis and workup of sarcoidosis: Focus on atypical manifestations. *RadioGraphics*. 2018;38:1536-49. doi: 10.1148/rg.2018180053.
- Ortega IH, González LL. Update thoracic sarcoidosis. *Radiología*. 2011;53(5):434-48. doi:10.1016/j.rx.2011.03.010.
- Silva M, Nunes H, Valeyre D, Sverzellati N. Imaging of sarcoidosis. *Clinic Rev Allerg Immunol*. 2015;49:45-53. doi: 10.1007/s12016-015-8478-7.
- Nunes H, Brillet PY, Valeyre D, Brauner MW, Wells AU. Imaging in sarcoidosis. *Semin Respir Crit Care Med*. 2007;28(1):102-20. doi: 10.1055/s-2007-970336.
- Nunes H, Uzunhan Y, Gille T, Lamberto C, Valeyre D, Brillet PY. Imaging of sarcoidosis of the airways and lung parenchyma and correlation with lung function. *Eur Respir J*. 2012;40:750-65. doi: 10.1183/09031936.00025212.
- Spagnolo P, Sverzellati N, Wells AU, Hansell DM. Imaging aspects of the diagnosis of sarcoidosis. *Eur Radiol*. 2014;24:807-16. doi: 10.1007/s00330-013-3088-3.
- Keijsers RG, Veltkamp M, Grutters JC. Chest imaging. *Clin Chest Med*. 2015;36:603-19. doi: 10.1016/j.ccm.2015.08.004.
- Hawtin KE, Roddie ME, Mauri FA, Copley SJ. Pulmonary sarcoidosis: the 'Great Pretender'. *Clin Radiol*. 2010;65:642-50. doi:10.1016/j.crad.2010.03.004.
- Criado E, Sánchez M, Ramírez J, Arguis P, de Caralt TM, Perea RJ, et al. Pulmonary sarcoidosis: typical and atypical manifestations at high-resolution CT with pathologic correlation. *RadioGraphics*. 2010;30:1567-86. doi: 10.1148/rg.306105512.
- Conant EF, Glickstein MF, Mahar P, Miller WT. Pulmonary sarcoidosis in the older patient: conventional radiographic features. *Radiology*. 1988;169(2):315-9. doi: 10.1148/radiology.169.2.3174979.
- Nunes H, Humbert M, Capron F, Brauner M, Sitbon O, Battesti JP, et al. Pulmonary hypertension associated with sarcoidosis: mechanisms, haemodynamics and prognosis. *Thorax*. 2006;61:68-74. doi: 10.1136/thx.2005.042838.
- Walsh SL, Wells AU, Sverzellati N, Keir GJ, Calandriello L, Antoniou KM, et al. An integrated clinico-radiological staging system for pulmonary sarcoidosis: a case-cohort study. *Lancet Respir Med*. 2014;2(2):123-30. doi: 10.1016/S2213-2600(13)70276-5.
- Rosen Y, Moon S, Huang CT, Gourin A, Lyons HA. Granulomatous pulmonary angiitis in sarcoidosis. *Arch Pathol Lab Med*. 1977;101:170-4.
- Takemura T, Matsui Y, Saiki S, Mikami R. Pulmonary vascular involvement in sarcoidosis: a report of 40 autopsy cases. *Hum Pathol*. 1992;23:1216-23. doi: 10.1016/0046-8177(92)90288-e.
- Hoffstein V, Ranganathan N, Mullen JB. Sarcoidosis simulating pulmonary veno-occlusive disease. *Am Rev Respir Dis*. 1986;134:809-11. doi: 10.1164/arrd.1986.134.4.809.
- Jones RM, Dawson A, Jenkins GH, Nicholson AG, Hansell DM, Harrison NK. Sarcoidosis-related pulmonary veno-occlusive disease presenting with recurrent haemoptysis. *Eur Respir J*. 2009;34:517-20. doi: 10.1183/09031936.00044609.
- Corte TJ, Wells AU, Nicholson AG, Hansell DM, Wort SJ. Pulmonary hypertension in sarcoidosis: A review. *Respirology*. 2011;16:69-77. doi: 10.1111/j.1440-1843.2010.01872.x
- Simonneau G, Gatzoulis MA, Adatia I, Celermajer D, Denton C, Ghofrani A, et al. Updated clinical classification of pulmonary hypertension. *J Am Coll Cardiol*. 2013;62(25 suppl):D34-D41. doi: 10.1016/j.jacc.2013.10.029
- Aluja-Jaramillo F, Gutiérrez FR, Díaz-Telli F, Yevenes-Aravena S, Javidan-Nejad C, Bhalla S. Approach to pulmonary hypertension: From CT to clinical diagnosis. *Radiographics*. 2018;38(2):357-73. doi: 10.1148/rg.2018170046.
- Koo HJ, Chae EJ, Kim JE, Kim EY, Oh SY, Hwang HJ. Presence of macronodules in thoracic sarcoidosis: prevalence and computed tomographic findings. *Clin Radiol*. 2015;70(8):815-21. doi: 10.1016/j.crad.2015.03.012.
- Koyama T, Ueda H, Togashi K, Umeoka S, Kataoka M, Nagai S. Radiologic manifestations of sarcoidosis in various organs. *RadioGraphics*. 2004;24(1):87-104. doi: 10.1148/rg.241035076.
- Müller NL, Kullnig P, Miller RR. The CT findings of pulmonary sarcoidosis: analysis of 25 patients. *AJR Am J Roentgenol*. 1989;152(6):1179-82. doi: 10.2214/ajr.152.6.1179.
- Hamper UM, Fishman EK, Khouri NF, Johns CJ, Wang KP, Siegelman SS. Typical and atypical CT manifestations of pulmonary sarcoidosis. *J Comput Assist Tomogr*. 1986;10(6):928-36. doi: 10.1097/00004728-198611000-00006
- Crystal RG, Roberts WC, Hunninghake GW, Gadek JE, Fulmer JD, Line BR. Pulmonary sarcoidosis: a disease characterized and perpetuated by activated lung T-lymphocytes. *Ann Intern Med*. 1981;94:73-94. doi: https://doi.org/10.7326/0003-4819-94-1-73
- Bonham CA, Streck ME, Patterson KC. From granuloma to fibrosis: sarcoidosis associated pulmonary fibrosis. *Curr Opin Pulm Med*. 2016;22(5):484-91. doi:10.1097/MCP.0000000000000301.
- Patterson KC, Streck ME. Pulmonary fibrosis in sarcoidosis. Clinical features and outcomes. *Annals ATS*. 2013;10(4):362-70. doi: 10.1513/AnnalsATS.201303-069FR.
- Gerke AK. Morbidity and mortality in sarcoidosis. *Curr Opin Pulm Med*. 2014;20(5):472-8. doi: 10.1097/MCP.0000000000000080
- Viskum K, Vestbo J. Vital prognosis in intrathoracic sarcoidosis with special reference to pulmonary function and radiological stage. *Eur Respir J*. 1993;6:349-53.
- Shlobin OA, Nathan SD. Management of end-stage sarcoidosis: pulmonary hypertension and lung transplantation. *Eur Respir J*. 2012;39(6):1520-33. doi: 10.1183/09031936.00175511
- Abehsera M, Valerye D, Greiner P, Jaillet H, Battesti JP, Brauner MW. Sarcoidosis with pulmonary fibrosis: CT patterns and correlation with pulmonary function. *AJR Am J Roentgenol*. 2000;174(6):1751-7. doi: 10.2214/ajr.174.6.1741751.
- Grenier P, Valeyre D, Cluzel P, Brauner MW, Lenoir S, Chastang C. Chronic diffuse interstitial lung disease: diagnostic value of chest radiography and high-resolution CT. *Radiology*. 1991;179:123-32. doi: 10.1148/radiology.179.1.2006262.
- Grenier P, Chevret S, Beigelman C, Brauner MW, Chastang C, Valeyre D. Chronic diffuse infiltrative lung disease: determination of the diagnostic value of clinical data, chest radiography, and CT with Bayesian analysis. *Radiology*. 1994;191:383-90. doi: 10.1148/radiology.191.2.8153310.
- Balan A, Hoey ETD, Sheerin F, Lakkaraju A, Chowdhury FU. Multi-technique imaging of sarcoidosis. *Clin Radiol*. 2010;65:750-60. doi: 10.1016/j.crad.2010.03.014.
- Nakatsu M, Hatabu H, Morikawa K, Uematsu H, Ohno Y, Nishimura K, et al. Large coalescent parenchymal nodules in pulmonary sarcoidosis: "sarcoid galaxy" sign. *AJR Am J Roentgenol*. 2002;178(6):1389-93. doi: 10.2214/ajr.178.6.1781389.
- Gotway MB, Tchao NK, Leung JW, Hanks DK, Thomas AN. Sarcoidosis presenting as an enlarging solitary pulmonary nodule. *J Thorac Imaging*. 2001;16(2):17-22. doi: 10.1097/00005382-200104000-00010.
- Herráez Ortega I, Alonso Orcajo N, López González L. The "sarcoid cluster sign": a new sign in high resolution chest CT [in Spanish]. *Radiología*. 2009;51(5):495-9. doi: 10.1016/j.rx.2009.05.003.
- Polychronopoulos VS, Prakash UBS. Airway involvement in sarcoidosis. *Chest*. 2009;136:1371-80. doi: 10.1378/chest.08-2569.
- Aluja-Jaramillo F, Gutiérrez FR, Rossi S, Bhalla S. Nonneoplastic tracheal abnormalities on CT. *Contemp Diagn Radiol*. 2020;43;13:1-7. doi: 10.1097/01.CDR.0000668640.54833.06
- Park HJ, Jung JI, Chung MH, Song SW, Kim HL, Baik JH, et al. Typical and Atypical Manifestations of Intrathoracic Sarcoidosis. *Korean J Radiol*. 2009;10:623-631. doi: 10.3348/kjr.2009.10.6.623.
- Soskel NT, Sharma OP. Pleural involvement in sarcoidosis: case presentation and detailed review of the literature. *Semin Respir Med*. 1992;13(6):492-514.
- Lynch JP III, Kazerooni EA, Gay SE. Pulmonary sarcoidosis. *Clin Chest Med*. 1997;18(4):755-85. doi: 10.1016/s0272-5231(05)70417-2.
- Jarman PR, Whyte MK, Sabroe I, Hughes JM. Sarcoidosis presenting with chylothorax. *Thorax*. 1995;50(12):1324-5. doi: 10.1136/thx.50.12.1324
- Blankstein R, Waller AH. Evaluation of known or suspected cardiac sarcoidosis. *Circ Cardiovasc Imaging*. 2016;9:e008867. doi: 10.1161/CIRCIMAGING.113.000867
- Birnie DH, Sauer WH, Bogun F, Cooper JM, Culver DA, Duvernoy S, et al. HRS expert consensus statement on the diagnosis and management of arrhythmias associated with cardiac sarcoidosis. *Heart Rhythm*. 2014;11:1305-23. doi: 10.1016/j.hrthm.2014.03.043.
- Sobic-Saranovic D, Artiko V, Obradovic V. FDG PET imaging in sarcoidosis. *Semin Nucl Med*. 2013;43(6):404-11. doi: 10.1053/j.semnuclmed.2013.06.007.
- Teirstein AS, Machac J, Almeida O, Lu P, Padilla ML, Iannuzzi MC. Results of 188 whole-body fluorodeoxyglucose positron emission tomography scans in 137 patients with sarcoidosis. *Chest*. 2007;132:1949-53.
- Krüger S, Buck AK, Mottaghy FM, Pauls S, Schelzig H, Hombach V, et al. Use of integrated FDG-PET/CT in sarcoidosis. *Clin Imaging*. 2008;32(4):269-73. doi:10.1016/j.clinimag.2007.11.005

53. Love C, Tomas MB, Tronco GG, Palestro CJ. FDG PET of infection and inflammation. *RadioGraphics*. 2005;25:1357-68. doi: 10.1148/rg.255045122.
54. Braun JJ, Kessler R, Constantinesco A, Imperiale A. 18F-FDG PET/CT in sarcoidosis management: review and report of 20 cases. *Eur J Nucl Med Mol Imaging*. 2008;35:1537-43. doi 10.1007/s00259-008-0770-9

## Correspondence

Felipe Aluja-Jaramillo  
Departamento de Radiología  
Hospital Universitario San Ignacio  
Carrera 7 # 40-62  
falujaj@husi.org.co

Received for evaluation: August 19, 2020

Accepted for publication: December 14, 2020